# Optimisation of district heating transformation for the efficient integration of a low-temperature heat source

Jan Stock[a,*], Till Schmidt[a], André Xhonneux[a], Dirk Müller[a,b]

[a] *Institute of Energy and Climate Research - Energy Systems Engineering (IEK-10), Forschungszentrum Jülich GmbH, Wilhelm-Johnen-Straße, 52425 Jülich*
[b] *Institute for Energy Efficient Buildings and Indoor Climate, E.ON Energy Research Center, RWTH Aachen University, Mathieustraße 10, 52074 Aachen*

**Abstract**

Reducing greenhouse gas emissions is becoming increasingly important, especially for energy systems that supply heat. District heating networks are a promising way to supply heat to buildings with low greenhouse gas emissions, especially with integrated low-temperature heat sources from renewables or waste heat. However, integrating low-temperature heat sources into existing district heating systems often requires a transformation to lower network temperatures. Promising approaches to reduce the network temperatures are the installation of central and decentral heat pumps and the refurbishment of the supplied buildings. In this paper, we present an optimisation model that considers refurbishment options for buildings and the installation of heat pumps to optimise the integration of low-temperature heat sources into existing district heating systems. The presented methodology is applied to a real-world high-temperature district heating system. Compared to conventional waste heat integration with only a central heat pump, the consideration of optional decentral heat pumps reduces the total annualised cost by 6.4 % and the additional consideration of building refurbishment options reduces the costs by 24.4 %. Overall, the network temperatures at nominal supply could be reduced by about 50 K due to the adaptions made to the most critical buildings in the existing district

*Corresponding author
*Email address:* j.stock@fz-juelich.de (Jan Stock )

heating system. The presented optimisation model shows the importance to also include decisions on building refurbishment in the overall district heating transformation process to achieve efficient integration of low-temperature heat sources.

*Keywords:* District Heating, Transformation, Building Refurbishment, Heat Pump Integration, Waste Heat Usage, Optimisation, Simulation

## 1. Introduction

Reducing greenhouse gas emissions to near zero is a medium-term goal for industry and politics throughout the European Union [1]. The total amount of greenhouse gas emissions is particularly influenced by the energy sector, which accounted for 31.4 % in the European Union in 2020 [2]. The residential sector was responsible for 28 % of final energy consumption, which was mainly for space heating [2]. However, 56 % of space heating demand was met by fossil fuels [3]. Therefore, fossil fuel heating in the residential sector must be replaced by sustainable heat sources to reduce greenhouse gas emissions. District heating (DH) systems offer great potential for distributing the heat from sustainable heat sources such as waste heat or renewable energy sources. However, in 2020, more than 90 % of DH networks were still supplied by fossil-based heat sources [4].

Analysing the DH network temperature level is crucial for the utilisation of sustainable heat sources, since most renewable and waste heat sources are available at a low-temperature level, such as rivers or lakes [5], geothermal heat [4] or excess heat from high-performance computers [6]. A general definition of DH systems and their corresponding temperature levels is given by [7]. Accordingly, the 1st generation is operated with steam as a heat transfer medium at temperatures close to 200 °C. The supply temperatures of the 2nd generation or high-temperature district heating (HTDH) systems are above 100 °C, while the 3rd generation systems operate below 100 °C. 4th generation or low-temperature district heating (LTDH) systems are characterised by temperature levels below 70 °C [7]. Not only the possibility of using low-temperature heat

sources is advantageous, but low DH supply temperatures also increase the efficiency of system components such as heat pumps (HP) or combined heat and power plants [8]. However, most existing DH systems operate with high supply temperatures and only a small share of sustainable heat sources and can therefore be classified as 2nd and 3rd generation of DH [4]. For that reason, these outdated HTDH systems need to be transformed to lower supply temperatures, i.e. to recent DH generations, to benefit from the usage of low-temperature sustainable heat sources and an overall increase of DH operating efficiency. However, the transformation of existing DH systems to lower supply temperatures faces several challenges and limitations. The following literature review gives an overview of the DH transformation process and supporting simulation and optimisation approaches for evaluation.

### *1.1. Literature review*

Several studies summarise the necessary measures for DH transformation, such as lowering the network supply temperature, integrating sustainable heat sources and storage systems as well as introducing smart metering and control devices [9, 10]. Different strategies for transformation are given by [11, 12] while [13] provides some helpful indicators for evaluating the DH transformation process.

As most existing DH systems are supplied by fossil-based heating plants, the main aim of DH transformation is the integration of sustainable heat sources. The possibility for integrating sustainable heat sources into existing DH systems is frequently investigated [14, 15, 16, 17]. However, the main barrier is mostly the difference between the temperature levels of the network and the available heat source. Therefore, the efficient compensation of the different temperature levels by reducing network temperatures [8, 10] and implementing boosting options at critical points in the DH system [18, 10] is crucial for DH transformation. In general, the implementation of temperature reduction and compensation measures is beneficial for any existing district heating system, even without the intention of integrating low-temperature heat sources, as heat

losses are reduced, which results in more efficient DH operation [19, 20].

According to Guelpa et al. [8], reducing the supply temperature of a DH system without extensive measures is limited by three subsystems of the DH system, namely the existing pipe network, the space heating (SH) system and the associated substations of the supplied buildings. They found that DH supply temperature reductions of 5-10 °C are possible in most cases without extensive measures, e.g. by fixing faults at the substations of the supplied buildings. In many case, the over-dimensioning of existing DH components, e.g. oversized pipes or substations, allows the sufficient heat supply despite reduced supply temperatures [8]. Several studies showed that the exploitation of over-dimensioning is often limited with respect to the SH systems of the supplied buildings, more specifically to the installed radiators in the rooms [8, 21, 22]. Østergaard et al. [23] conclude that for most supplied SH systems, DH supply temperatures below 55 °C are sufficient for most of the year to ensure the comfort of the end users. Only at very low ambient air temperatures, the supply temperatures need to be higher to ensure sufficient heat supply [23].

To achieve further supply temperature reductions at the SH systems of the buildings, critical radiators that limit a further temperature reduction must be replaced [24, 21]. A detailed simulation study by [25] showed that replacing critical radiators can reduce the required supply temperature at the SH system by about 5-10 °C. However, the proportion of critical radiators varies depending on the aspired temperature reduction and the particular building [25]. In addition, the overall refurbishment of the buildings is another way to reduce the required SH supply temperatures. Refurbishing buildings reduces their nominal heating loads, which also reduces the required supply temperature of their SH systems [26, 21]. However, to achieve the aimed SH system temperature reduction through refurbishment, additional replacement of a few critical radiators might still be necessary [26].

Dynamic simulation models are a common approach to estimate the possible heating load reduction in existing buildings through refurbishment measures and the accompanying supply temperature reduction. Harrestrup et al. [27] showed

that reductions in the nominal heating load of up to 72 % are possible through a comprehensive refurbishment of the building envelope. They used dynamic building simulation to analyse the effects of different refurbishment stages of Danish multi-story buildings from 1910 and 1906. Brand et al. [28] and Wang et al. [29] presented similar results also using dynamic building simulations. They showed that reductions of up to 50-55 % of the heating demand and reductions of up to 10 °C of the supply temperature are possible for typical Danish single-family houses from 1970 [28] and Swedish multi-family houses from 1965-1975 [29].

For the integration of low-temperature heat sources in HTDH systems, the installation of central and decentral HPs is beneficial to compensate for different temperature levels [30, 18, 31]. Capone et al. [32] investigated the installation of a large-scale HP into an existing HTDH system and showed a potential for $CO_2$ reduction of 4 %. Another study conducted by [33] evaluated the integration of large-scale HPs into transmission and distribution DH networks and showed that HPs can displace peak loads during winter time but their full load operating time depends on the network type. Different HP configurations in a DH system were analysed by [18], pointing out that a beneficial HP installation, for instance to increase domestic hot water temperature in a decentral manner, can improve the overall efficiency of a DH system. Hering et al. [30] presented a methodology for designing a LTDH system and showed that combining central and decentral HPs for low-temperature heat source utilisation can reduce costs and $CO_2$ emissions.

In the context of DH systems, the use of optimisation approaches is widespread in current research [34]. In particular, mixed integer linear programming (MILP) is widely used to model and optimise thermal distribution networks [35, 30, 36]. Since DH systems have temperature and mass flow dependent energy flows and temperature dependent component efficiencies, bilinear formulations can be of great benefit [37]. Adding bilinear terms to a MILP formulation, which leads to mixed integer quadratic constrained programming (MIQCP), ensures that the models accurately depict real-world components [38, 30].

The reviewed literature addresses various approaches to transform exist-

ing DH systems by integrating sustainable heat sources and reducing supply temperatures. To achieve DH transformation, measures are taken either on the DH system level or at the building level. However, there is no literature that addresses the integration of a low-temperature heat source and the overall DH system design adaption that simultaneously includes building refurbishment measures and HP installation.

### *1.2. Contribution*

The DH transformation in this work focuses on integrating a low-temperature heat source into a HTDH system, whereby the optimal measures for reducing DH supply temperatures are determined. Therefore, this work aims to model the transformation of an existing DH system as a mathematical optimisation problem and to optimise the integration of low-temperature heat sources into the network structure. For this purpose, the refurbishment of supplied buildings and the installation of central and decentral HPs are considered in the problem formulation.

Previous work on optimising DH systems mainly focused on designing new DH systems [30, 35, 36] or optimising the operation of an existing DH system [36, 37]. However, the optimisation of existing DH systems in this work analyses the additional integration of a newly utilised heat source while simultaneously optimising the decision to integrate a HP or to refurbish the existing buildings. The presented optimisation problem to analyse DH transformation uses models from previous work [30], which are partially extended in this work to analyse DH transformation, e.g. to consider refurbishment options at existing buildings that influence heat demand and temperature requirements.

For the constructed optimisation problem, different refurbishment packages are considered for each existing building in the DH system. Therefore, the effects of building refurbishment on the heat demand and on the temperature requirements of the installed heating systems are evaluated individually for each building using dynamic simulation models. These optional refurbishment packages and their impact on the buildings are then considered when optimising the

DH transformation.

To demonstrate the applicability of the developed model, the optimisation problem is applied to a real-world HTDH system with an intended low-temperature waste heat utilisation. This DH transformation analysis focuses on a supply temperature reduction to enable the most efficient integration of the low-temperature heat source, which, however, may not ultimately reach the temperature levels that characterise a LTDH system.

This paper is structured as follows: Section 2 describes the methodology used. At first, the evaluation of the refurbishment measures on existing buildings and, second, the formulation of the optimisation problem. The case study under consideration is described in Section 3. The results are presented in Section 4, followed by a discussion in Section 5 on the presented methodology and the obtained results. Finally, Section 6 concludes the work and gives a short outlook.

## 2. Methodology

This section first describes the analysed measures to transform existing DH systems in Section 2.1. Second, the optimisation problem, including formulations of DH system components, is given in Section 2.2.

### *2.1. Transformation of existing DH systems*

This study investigates the transformation of DH systems with regard to the integration of low-temperature heat sources. Two measures for the transformation of DH systems are considered: The refurbishment of supplied buildings and the installation of central and decentral HPs to compensate different temperature levels.

#### *2.1.1. Refurbishment of buildings*

The refurbishment of the building envelope reduces the heat losses of the building and, thus, also the heating load of the SH system. Through the reduced heating load, the required supply temperature of the SH system can also

be reduced [26, 21]. To analyse the effects of the refurbishment on the heating load and required supply temperature, three different building states are considered. The first state represents the present building without refurbishments (Benchmark). The second state $\text{Refurb}_{\text{Win}}$ describes a refurbishment state in which all windows of the building are replaced. The third state $\text{Refurb}_{\text{Full}}$ symbolises an holistic refurbishment of the building, in which the windows are replaced and the envelope is insulated. The states of the buildings are shown in Table 1.

Table 1: Different building states and considered refurbishment measures in each state.

| Measure | Benchmark | $\text{Refurb}_{\text{Win}}$ | $\text{Refurb}_{\text{Full}}$ |
|---|---|---|---|
| Window replacement | | x | x |
| Envelope insulation | | | x |

The effects of both refurbishment packages ($\text{Refurb}_{\text{Win}}$ and $\text{Refurb}_{\text{Full}}$) on the heating load and required supply temperature are evaluated in relation to the present building state (Benchmark) by dynamic simulation models. The generation of the simulation models for each building and its three possible states is automated with the tool *TEASER* [39]. *TEASER* is a tool to generate dynamic simulation models of typical buildings with minimal input data, such as the year of construction and the net leased area. Based on the input data provided, statistical data is used to enrich the building models that are generated in the modeling language Modelica [39]. An implemented function of *TEASER*, which applies the refurbishment measures (Table 1) to the building model, is used to create the corresponding building models for each building state. For each building and its three states, one-year simulations are performed with an hourly resolution. Thus, the simulation results allow the evaluation of the relative heating load reduction between the different building states.

The simulated heating loads of all building states are used to estimate the relative supply temperature reduction of the SH system after refurbishment. A

method proposed by Lämmle et al. [26] showed that a comparison of the nominal heating load before the refurbishment $\dot{Q}_{nom,1}$ and after the refurbishment $\dot{Q}_{nom,2}$ can be used to estimate a reduced supply temperature $T_{sup,2}$ of the existing SH system within the building:

$$T_{sup,2} = T_{room} + \Delta T_2 \frac{exp\left(\frac{\Delta T_2}{\Delta T_{log,2}}\right)}{exp\left(\frac{\Delta T_2}{\Delta T_{log,2}}\right) - 1}, \tag{1}$$

with

$$\Delta T_2 = (T_{sup,1} - T_{ret,1}) \frac{\dot{Q}_{nom,2}}{\dot{Q}_{nom,1}}, \tag{2}$$

where $T_{room}$ is the required room temperature, $T_{sup,1}$ and $T_{ret,1}$ are the supply and return temperatures before the refurbishment and $\Delta T_{log,2}$ is the logarithmic temperature difference. In [26], the method is applied to real-world case studies showing that up to 10 % of the total number of radiators are still critical after refurbishment and need to be replaced to ensure an operation at the reduced supply temperature $T_{sup,2}$.

The method proposed by Lämmle et al. [26] is used in this study to estimate the possible supply temperature reduction of the SH system if the building is refurbished. The calculations of the possible supply temperature reduction are based on the reduced nominal heating load resulting from the simulations and linked to the corresponding refurbishment states $\text{Refurb}_{\text{Win}}$ and $\text{Refurb}_{\text{Full}}$. An assumed critical radiator replacement rate of 10 % according to [26] is considered for the application of a refurbishment package.

The costs associated with each refurbishment measure are estimated and considered individually for each studied building. The cost functions for material and implementation [40] are applied to the corresponding measures in Table 1 and the radiator replacement. The used cost functions are summarised in Table A.4 in the Appendix.

In summary, the simulation study estimates the reduced SH heating load of an existing building for two considered refurbishment packages. Based on these heating load reductions, a reduced supply temperature is derived. Finally, the

costs of each refurbishment measure are calculated based on individual building data.

### *2.1.2. Installation of HPs*

Usually, different temperature levels of low-temperature heat sources and the existing DH networks are compensated by using a central HP. However, reducing network temperatures is helpful to increase the DH efficiency as heat losses are reduced and the central HP operates more efficiently due to the lower temperature difference between the heat source and the network. If the network temperature is reduced below the required supply temperature of some supplied buildings, the installation of decentral HPs at these buildings is useful to meet temperature requirements, either in conjunction with building refurbishment or without.

Central HPs have lower specific costs than smaller decentral HPs [41] but they have to increase the supply temperature with regard to the most critical building in the DH system. Decentral HPs with mostly smaller thermal capacities have higher specific costs but can raise the supply temperature to the local conditions as required [30, 18, 41]. Both options for HP installation are considered within this study as measures for DH transformation. The costs of central and decentral HPs are described in the component formulations of the optimisation problem in Section 2.2.3.

## *2.2. Optimisation of DH system transformation*

The optimisation model is developed using the object-oriented modeling framework *COMANDO* [42]. The used models are partly based on previous work [30]. The model formulations are extended and adapted to describe HTDH systems and to consider building refurbishment options. Figure 1 shows the superstructure of the DH system.

The heating station (HS) represents an existing high-temperature heating plant and is connected to the network with a central heat exchanger (HX). The low-temperature heat source is assumed to be a waste heat (WH) source. The

WH and the consumers (C), i.e. the supplied buildings, are connected to the network by a so-called linking component (LC). The LCs contain both a HP and a HX model with the corresponding decision variables to build either a HX or a HP. The decentral LCs do not take into account costs for building a HX, as they are already present in the existing DH system. All build HPs are connected to the power grid (PG).

The operation of the DH system is primarily temperature dependent. To account for the different temperature levels within the DH system, bilinear terms are used to describe the components HP, HX, and network (NET). The use of bilinear terms leads to quadratic constraints and therefore to a MIQCP [30].

The various model components are explained in more detail in the following. Therefore, Figure 2 shows the principle of model component construction according to [30], exemplarily for HP, HX and NET. Each component consists of a supply side $a$ and a demand side $b$ with corresponding connectors. For HPs,

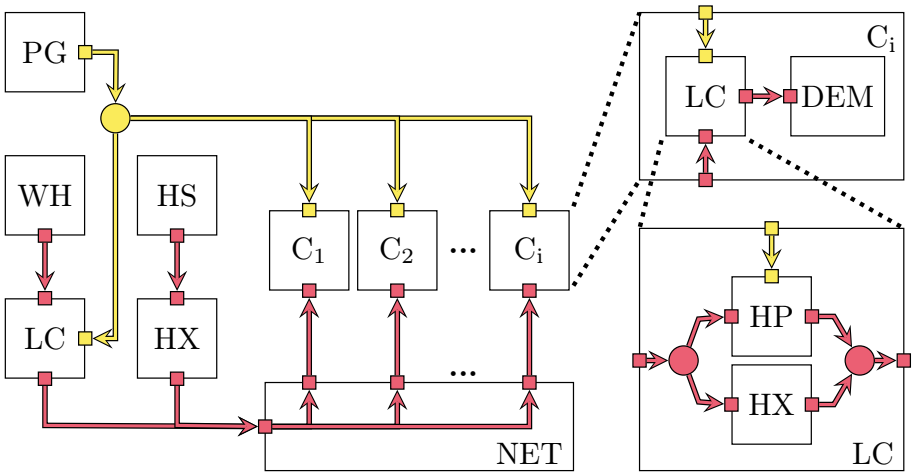



Figure 1: Superstructure of the DH system with yellow connections representing power flows from the power grid (PG) and red connections representing heat flows. A heating station (HS) and a waste heat (WH) source form the heat supply. The DH network is represented by the network (NET) component. Each consumer (C) consists of a corresponding heat demand (DEM) and a linking component (LC). Each LC consists of a heat exchanger (HX) and a heat pump (HP).

side $a$ corresponds to the evaporator and side $b$ to the condenser. Each side has an input temperature $T_{in}$ and an output temperature $T_{out}$. The mass flows and temperatures are indexed to side $a$ and $b$ if they differ between the sides.

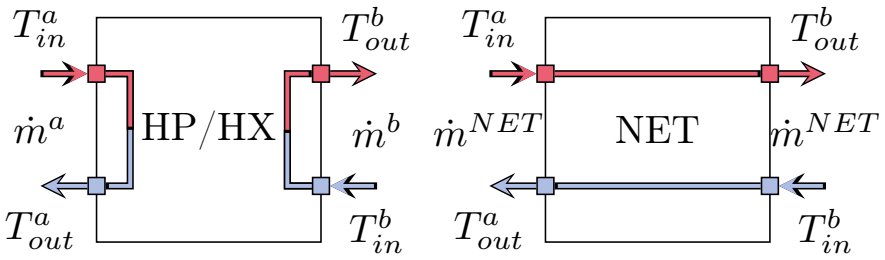



Figure 2: Connectors of the NET, HP and HX models. The temperatures and mass flows are indexed to side $a$ and $b$.

### *2.2.1. Network model*

The network model is formulated similarly to previous work [30]. The network model considers the heat losses that occur when optimising the DH temperature level. Side $a$ is the supply side of the DH network, connected to the HS and the WH. Side $b$ is the consumer side, connected to all consumers $c \in C$.

The temperature difference $\Delta T^{NET,b}$ between $T^{NET,b}_{out,t}$ and $T^{NET,b}_{in,t}$ at side $b$ is assumed to be constant over time. The fixed temperature difference is a reasonable simplification of the energy balance at the consumer side $b$ and used in previous work [30, 42]. The effect of different values for $\Delta T^{NET,b}$ is analysed in Section 4.2.1.

As the return temperatures in a DH network are often not reduced as much as the supply temperatures, the temperature difference between supply and return decreases, resulting in increasing mass flows in the pipe network to satisfy the heat supply [8]. Therefore, the resulting mass flow limits for each pipe segment are calculated to identify too high mass flows due to reduced temperatures. The maximum allowed mass flows are calculated according to [43], taking into account a specific pressure difference of 250 Pa/m. The mass flow of the DH network $\dot{m}^{NET}_t$ is constrained by the maximum possible mass flow for the

overall network structure $\dot{m}_{max}^{NET}$. However, the calculated mass flow limits for individual pipes are not used as constraints in the optimisation model, since pipe segments can tolerate time-limited mass flow exceedances. Therefore, the critical pipe segments that exceed the mass flow limits are analysed in a post-processing step.

*2.2.2. Consumer model*

The consumer model C contains an LC and a DEM model (see Figure 1), which is derived from [30]. The DEM symbolises the SH system, taking into account the heat demand of the building and the required supply temperature. The DEM model considers two optional refurbishment packages (see Table 1) and, thus, adds two decision variables $b_{refurb,1}$ and $b_{refurb,2}$ to the model. Since only one refurbishment package can be applied to a consumer, the decision variables are constrained by

$$b_{refrub,1} + b_{refurb,2} \quad \leq \quad 1. \tag{3}$$

This refurbishment decision affects the heat demand $\dot{Q}_t^{DEM}$ and the required design supply temperature $T_{in,t}^{DEM}$ of the consumer according to the results derived from the dynamic building simulations described in Section 2.1.1.

The supply temperature $T_{in,t}^{DEM}$ is considered as a heat curve for each consumer individually. The heat curves are automatically adjusted when a refurbishment package is used based on data derived from section 2.1.1. The LC of the consumer model supplies heat directly to the DEM and adds two decision variables to the model, representing the decision to use an HP or an HX [30].

*2.2.3. Heat pump and heat exchanger model*

The formulations of the HP and HX model are taken from previous work [30]. The HP model uses formulations for part-load efficiencies that contain bilinear terms and thus add quadratic constraints to the model. Based on the design value of the thermal capacity $\dot{Q}_{design}^{HP}$, the investment $I$ is added to the HP model according to [41] with 670 EUR/kW for the central and 1300 EUR/kW

for the decentral HPs. Since we focus on the transformation of the DH system, no costs are considered for the decentral HX and the central HX at the HS, as they are already present in the current DH system. For the optional central HX at the WH, specific costs of 90 EUR/kW are assumed according to [44].

*2.2.4. Energy source models*

The WH and the HS are the two heat sources supplying the DH network. The WH is connected to the network through an LC, and the HS is connected to the network through an HX. The network supply temperature $T_{in,t}^{NET,a}$ at side $a$ must be equal to the supply temperature at both heat sources. Therefore equation (4) holds for each time step $t \in T$,

$$T_{in,t}^{NET,a} = T_{out,t}^{LC,b} = T_{out,t}^{HX,b}, \quad \forall t \in T \tag{4}$$

where $T_{out,t}^{LC,b}$ is the supply temperature of the LC connecting the WH and $T_{out,t}^{HX,b}$ is the supply temperature of the HS behind its HX. The sum of the outgoing mass flows $\dot{m}_{out,t}^{LC,b}$ and $\dot{m}_{out,t}^{HX,b}$ is equal to the mass flow of the DH network NET $\dot{m}_t^{NET}$. In addition, the PG is modeled as an unlimited power source supplying all HPs.

*2.2.5. Objective function*

The optimisation problem minimises an economic function based on operating costs and investments. Therefore, we calculated the total annualised costs (TAC) according to

$$\text{TAC} = \frac{(1+i)^n \cdot i}{(1+i)^n - 1} \cdot \text{CAPEX} + \text{OPEX}, \tag{5}$$

where $i$ is the assumed interest rate of 4 % and $n$ is the assumed time horizon of 20 years. Capital expenditures (CAPEX) consist of investments $I$ for the central HP $I_{central}^{HP}$ or HX $I_{central}^{HX}$ to enable WH utilisation, for all consumers $c$ optional decentral HPs $I_c^{HP}$, as well as investments for optional building refurbishment $I_c^{refurb}$. Since we focus on the transformation of existing DH systems we do not consider investments for the network or the supplying HS. Therefore, CAPEX

are calculated according to

$$\begin{aligned} \text{CAPEX} = I_{central}^{HP} + I_{central}^{HX} + \\ \sum_{c \in C} \Big[ I_c^{HP} + I_c^{refurb} \Big]. \end{aligned} \tag{6}$$

The operational expenditures (OPEX) depend on the power consumption of the HPs with corresponding costs $p_{el}$ and specific heat costs for HS heat supply $p_{heat}^{HS}$ and WH heat supply $p_{heat}^{WH}$ for each time step $t \in T$. Accordingly, OPEX are calculated according to

$$\begin{aligned} \text{OPEX} = \sum_{t \in T} w_t \cdot \Bigg[ p_{el} \cdot \Bigg( \sum_{c \in C} P_{el,t,c}^{HP} + P_{el,t,central}^{HP} \Bigg) \\ + p_{heat}^{HS} \cdot P_{heat,t}^{HS} + p_{heat}^{WH} \cdot P_{heat,t}^{WH} \Bigg], \forall t \in T, \end{aligned} \tag{7}$$

where $w_t$ is the weight of time step t, $P_{el,t}^{HP,c}$ is the power consumption of the HP of consumer $c$, $P_{el,t,central}^{HP}$ is the power consumption of the optional central HP, $P_{heat,t}^{HS}$ is the heat supply of the HS and $P_{heat,t}^{WH}$ is the heat supply of the WH.

## 3. Case study

The developed methodology can be applied to existing HTDH systems to show the optimal design of DH transformation. In this study, the presented methods are applied to an existing HTDH system of the research facility Forschungszentrum Jülich in Germany that supplies 92 buildings. The spatial distribution of the HTDH network is shown in Figure 3. The visualisation and the data handling of the DH network is done using *uesgrahps* [45], which is a Python-based energy network tool for organising and visualising network data.

The following building parameters are used to create the building simulation models: Year of construction, number of floors, height of floors, net leased area and the type of building usage. The building simulation models are used to derive the relative heating load and SH system temperature reductions of an optional refurbishment package. Based on these relative reductions, reduction

factors are calculated for each building and refurbishment package and applied to the available 2017 demand measurement data and individual heat curves of the buildings. Thus, optional refurbishment states could be derived for each supplied building in the DH system and incorporated into the optimisation model as a design decision.

Some of the buildings studied have a domestic hot water demand, which is however not supplied by the DH network and therefore does not affect the temperature requirements of the buildings. Any air conditioning systems installed in the supplied buildings are not considered in this study since the operation of these systems is very individual and no specific data is available. The limitation of supply temperature reduction imposed by an air conditioning system must be analysed individually in a real-world application.

Currently, a gas-fired HS supplies the DH system at a temperature level of $T^{HS}_{out,t}$=130 °C. An upcoming high-performance computer will serve as a WH source with a maximum thermal output of 18 MW that should be integrated into the DH system. The expected supply temperature $T^{WH}_{out,t}$ of the WH is 44 °C. Due to the difference between the supply temperatures of the DH network and the WH, a transformation of the DH system to lower supply temperatures is necessary to efficiently integrate the low-temperature waste heat.

The heat costs of the WH $p^{WH}_{heat}$ are zero. The heat costs of the gas-fired HS $p^{HS}_{heat}$ are derived from project data and set to 0.174 EUR/kWh. The costs of electricity $p_{el}$ are assumed to be constant with a specific electricity price of 0.25 EUR/kWh. Operating costs of the components, e.g. for maintenance, are not considered. All investments described in Section 2 are adjusted using inflation data from [46]. These prices are used to present a model application to a real-world HTDH system. Nevertheless, we would like to mention that changed prices, either for the HP installation, the refurbishment packages or for gas and electricity, may influence the optimisation results. However, since the focus of this work is on the developed optimisation model and the influence on the achievable supply temperature reduction in a DH system, the influence of economic boundary conditions is not analysed further in the scope of this work.

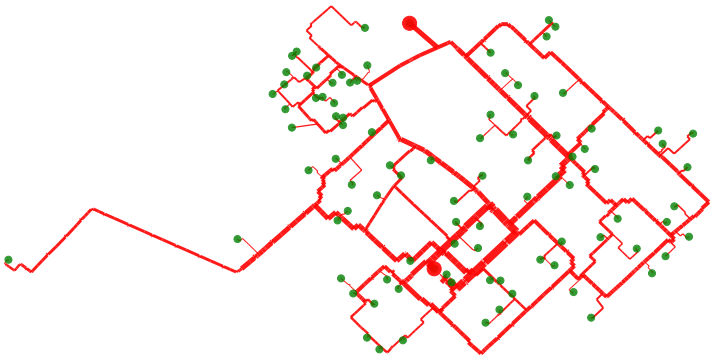


Figure 3: Model of the studied HTDH network. The green dots represent the connected buildings and the line thickness represents the pipe diameter. The heat sources are shown as red dots, the already connected WH source in the north of the network and the HS in the south of the network.

To reduce the model size and therefore the computational time, it is advantageous to separate the design and operational optimisation into a two-stage optimisation approach [47, 42]. First, the design optimisation is performed with typical operational points to determine the transformed design of the DH system under investigation, i.e. at which buildings HPs should be installed or a refurbishment package should be applied and what DH supply temperature reduction is possible with these design adaptions. Therefore, k-means clustering is used to aggregate the demand data and to derive typical operational points of the DH system. For the design optimisation presented here, seven typical operational points are determined using k-means clustering [48]. The clustering is based on the sum of all measured heat demands of the consumers $\sum_{c \in C} \dot{Q}_t^{DEM,c}$ and the ambient air temperature $T_{amb,t}$. Each clustered point has a corresponding weight $w_t$ representing the occurrence of this point within one year. For the design optimisation, an additional operating point with the maximum heat demand and a weight $w_t$ of zero is added to account for the required nominal capacities of the optional components.

Second, the operational optimisation focuses on the transformed DH system, i.e. the design of the DH system is fixed and the operational variables are

optimised. In this operational optimisation, the previously defined parameter $\Delta T^{NET,b}$, i.e. the temperature difference at the consumers, is also converted to an operational variable, which enables a more detailed temperature optimisation during this second optimisation step. As the design decisions are fixed during the operational optimisation, the model is less complex and a longer time series can be used for analysis. Therefore, the demand data of the DH system is clustered into ten typical days with an hourly resolution for operational optimisation [49].

To sum up, the design optimisation uses seven typical operational points to determine the measures required for DH transformation, while the operational optimisation uses ten typical days with hourly resolution to further optimise the temperature level of the transformed DH system.

## 4. Results

The results are divided into the evaluation of the refurbishment measures in Section 4.1 and the optimisation of the DH system in Section 4.2. Section 4.2 first describes the design optimisation of the DH system and ends with the operational optimisation.

### *4.1. Refurbishment measures*

The refurbishment packages are considered individually for each building, i.e. the reduction of heat demand and supply temperature, as well as the costs of refurbishment, are calculated specifically for each building. Figure 4 shows the average nominal heating load and supply temperature reduction for both refurbishment packages for all DH supplied buildings. For a comprehensive presentation of the results, the buildings are grouped by the decade of their construction year in Figure 4.

The upper part of Figure 4 shows the average reduction of the nominal heating load for the refurbishment states $\text{Refurb}_{\text{Win}}$ and $\text{Refurb}_{\text{Full}}$ relative to the building state Benchmark. In the case of $\text{Refurb}_{\text{Full}}$, it can be observed that the nominal heating load is reduced more for older buildings. However, the

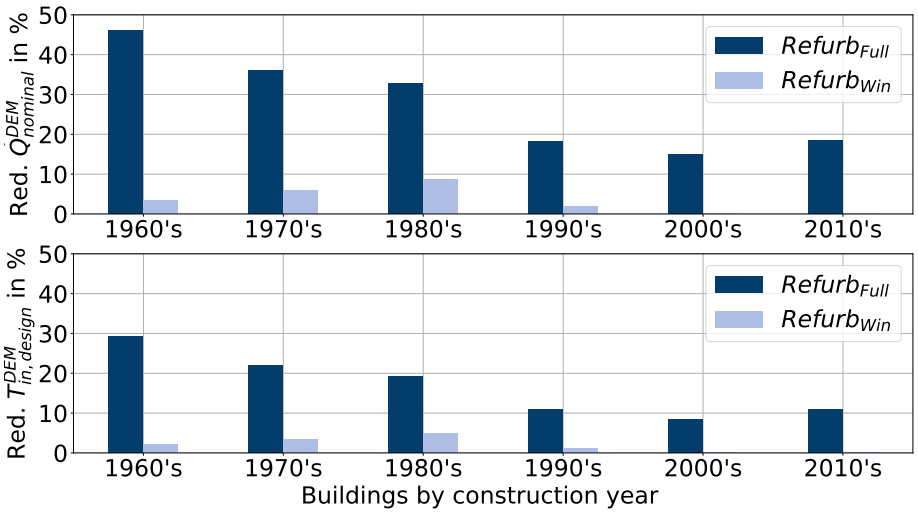



Figure 4: Average percentage reduction in heating load and supply temperature due to refurbishment measures grouped by year of construction of the buildings. The relative nominal heating load $\dot{Q}^{DEM}_{nominal}$ reduction is shown in the upper part, and the derived supply temperature $T^{DEM}_{in,design}$ reduction is shown in the lower part.

reduction is greater for buildings built in the 2010's than for buildings built in the 2000's, which can be explained by the fact that the proportion of building types, and thus their usage, varies with the decades in which the buildings were built. Since refurbishment affects office buildings differently than laboratories, the average reductions may be higher for recent decades. Comparing the two refurbishment states, $\text{Refurb}_{\text{Win}}$ shows a relatively smaller reduction in nominal heating load compared to $\text{Refurb}_{\text{Full}}$. In addition, the heating load reduction between the 1960's and 1980's buildings shows an opposite trend in the case of $\text{Refurb}_{\text{Win}}$ than in the case of $\text{Refurb}_{\text{Full}}$. This opposite reduction behaviour between the refurbishment packages could be due to different building standards in the different decades. In old buildings from the 1960's and 1970's with a poorly insulated envelope, the relative energy savings from refurbishing the windows are small compared to refurbishing the entire building envelope. With improved standards of envelope insulation in recent decades, the relative savings from window refurbishment become greater.

The lower part of Figure 4 shows the average reduction of the design supply temperature $T_{in,design}^{DEM}$ for both refurbishment states relative to the building state Benchmark. The same trends as in the upper part can be seen, since the calculation of relative $T_{in,design}^{DEM}$ reduction is based on the reduction of the nominal heating load $\dot{Q}_{nominal}^{DEM}$ (see Section 2.1.1).

### *4.2. Optimisation results*

The optimisation problems are solved with *Gurobi* 10.0.1 [50] on a machine with an Intel Core i7-9700 CPU and 8 physical and 8 logical processors. A time limit of 7200 s and an optimality gap of 1 % is set. Three scenarios are created for the presented case study to investigate the aimed DH transformation. The different configurations of the scenarios are shown in Table 2.

Table 2: Investigated optimisation scenarios and model configurations.

| Characteristic | $S_{Ref}$ | $S_{HP}$ | $S_{Refurb}$ |
|---|---|---|---|
| WH integration | HP | LC | LC |
| Decentral HPs | no | yes | yes |
| Refurbishment | no | no | yes |

The reference scenario $S_{Ref}$ symbolises the conventional low-temperature WH integration. A central HP is fixed to increase the temperature level centrally but no adaptions are possible on the consumer side, so the options for refurbishment and decentral HPs are disabled in $S_{Ref}$. Scenario $S_{HP}$ includes a central LC connected to the WH, so either integrating the WH through a central HP or HX, as well as LC components at the buildings for the option to build decentral HPs. However, refurbishment options are not considered in $S_{HP}$. Finally, scenario $S_{Refurb}$ consists of the same specifications as $S_{HP}$ with the additional option for building refurbishment.

*4.2.1. Design optimisation*

The design optimisation symbolises the first optimisation stage where the transformed DH design is determined. The design optimisation is performed with different values for the fixed temperature difference $\Delta T^{NET,b}$ between $T^{NET,b}_{out,t}$ and $T^{NET,b}_{in,t}$ at consumer side b of the DH network (see Section 2.2.1). Therefore, each scenario in Table 2 is optimised for different $\Delta T^{NET,b}$ values in a range of 10 to 25 K with 1 K increments, as all results with $\Delta T^{NET,b} >$ 25 K show steadily increasing TAC for each scenario. The results for all runs are summarised in Table A.5 for $S_{HP}$ and in Table A.6 for $S_{Refurb}$ in the Appendix.

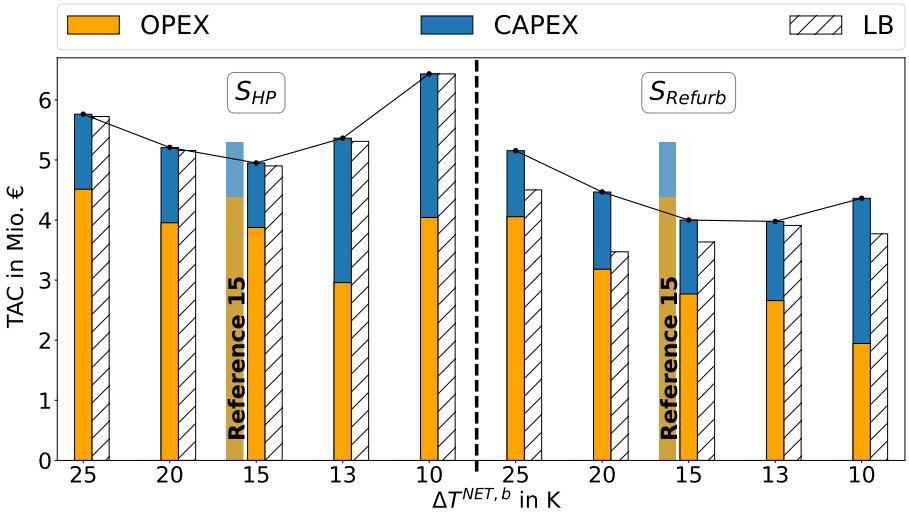



Figure 5: TAC of upper and lower bounds for different scenarios and $\Delta T^{NET,b}$ values. The left side shows scenario $S_{HP}$ and the right side $S_{Refurb}$. On both sides, scenario $S_{Ref}$ is shown with a $\Delta T^{NET,b}$ of 15 K. The blue and orange parts of the bars represent the CAPEX and OPEX respectively, which together give the upper bounds. Hatched white bars show the lower bounds (LB).

Figure 5 shows selected results for the different $\Delta T^{NET,b}$ runs. The TAC, differentiated between OPEX and CAPEX, is shown for scenario $S_{HP}$ on the left side and for $S_{Refurb}$ on the right side of Figure 5. The reference case $S_{Ref}$ is shown with a $\Delta T^{NET,b}$ of 15 K. The hatched white bars show the lower bounds (LB) of the scenarios given by the optimisation results. All results of $S_{Ref}$ and

$S_{HP}$ are solved within the time limit and the optimal gap of 1 %. However, no global optimality is proven for any $S_{Refurb}$. After 7200 s the gap varies between 1.7 % in $S_{Refurb,13}$ and 22.3 % in $S_{Refurb,20}$.

The share of CAPEX is higher in scenarios $S_{HP,13}$, $S_{HP,10}$ and $S_{Refurb,10}$ compared to other results. The increased investment in these three scenarios is due to a fully decentralised energy supply through decentral HPs in all buildings (see Table A.5 and Table A.6). The fully decentral HPs design of the DH system can be explained with the small $\Delta T^{NET,b}$, which limits the operation of a decentral HX. To operate a decentral HX with low $\Delta T^{NET,b}$ values, the mass flow of the network $\dot{m}_t^{NET}$ must be increased to account for the low $\Delta T^{NET,b}$. Since the total mass flow of the DH network $\dot{m}_t^{NET}$ is limited by $\dot{m}_{max}^{NET}$ (see Section 2.2.1), not all buildings can be supplied by the network when $\dot{m}_{max}^{NET}$ is reached. Therefore, decentral HPs are used to support the heat supply in scenarios with low $\Delta T^{NET,b}$.

Apart from these three fully decentral HPs designs ($S_{HP,13}$, $S_{HP,10}$ and $S_{Refurb,10}$), in all other scenarios shown in Figure 5 the design of the DH system is based on a central HP to integrate the WH and decentral adaptations at selected consumers.

As shown in Figure 5, the TAC results for $S_{HP,15}$ as well as for $S_{Refurb,15}$ and $S_{Refurb,13}$ are minimal. The HP scenario $S_{HP,15}$ reduces the TAC by 6.4 % compared to $S_{Ref,15}$. The refurbishment scenario $S_{Refurb,15}$ shows a reduction of 24.4 % compared to the reference scenario $S_{Ref,15}$. As $S_{HP,15}$ and $S_{Refurb,15}$ show minimal TAC and small gaps in both scenarios, these results are further analysed and verified. A detailed overview of the resulting HP installations and applied refurbishment packages for scenario $S_{HP,15}$ and $S_{Refurb,15}$ can be found in Table A.7 in the Appendix.

*DH design of $S_{HP,15}$*

In $S_{HP,15}$, the WH in combination with the central HP provides most of the heat supply to the DH network, but at high demand the HS supports the heat supply by up to 50 %. The resulting DH system design of scenario $S_{HP,15}$ is

shown in Figure 6 with six installed decentral HPs.




Figure 6: DH system design of scenario $S_{HP,15}$. Orange marked buildings represent decentral HP installations.

To investigate why these six buildings are selected for decentral HP installation, the heat curves of these critical buildings are further analysed. Figure 7 shows a sketch of three example heat curves $a$, $b$ and $c$. The supply temperature $T_{in}^{DEM}$ is shown on the y-axis and the ambient temperature $T_{amb}$ on the x-axis. $T_{in,max}^{DEM}$ in Figure 7 symbolises the design temperature $T_{in,design}^{DEM}$ of the heating system. The gradient of the heat curves is marked for each heat curve to illustrate the difference. Comparing heat curves $b$ and $c$, it can be seen that the lower gradient of b leads to higher supply temperatures $T_{in}^{DEM}$ at higher ambient temperatures $T_{amb}$. In addition, high supply temperatures $T_{in}^{DEM}$ can also occur for high ambient temperatures if the ambient temperature design point $T_{amb}^{min}$ is relatively high, which can be seen at heat curve $a$. Therefore, a low heat curve gradient or a high design ambient temperature $T_{amb}^{min}$ can lead to high temperature requirements in the buildings supplied.

Figure 8 shows all buildings in the DH system with respect to their gradients of the heat curves on the y-axis and their design supply temperatures $T_{in,design}^{DEM}$ on the x-axis. The gradients are multiplied by -1 to show a negative incline

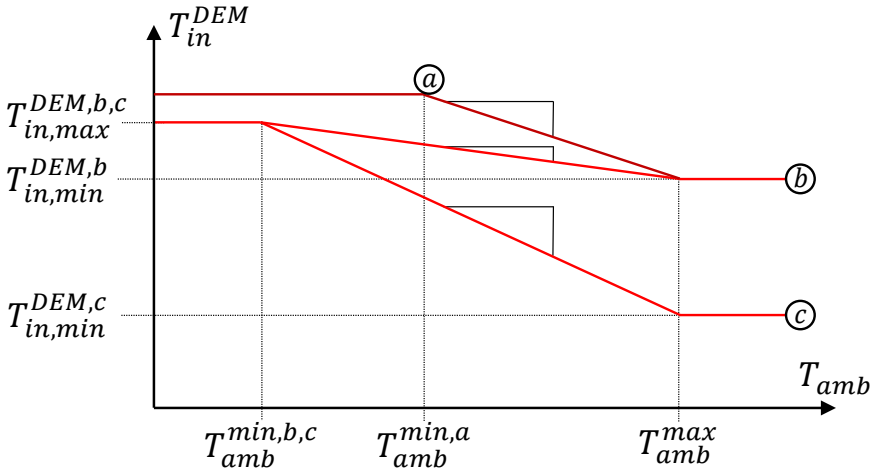



Figure 7: Sketch of three heat curves. Heat curve $a$ shows higher design ambient temperatures $T_{amb}^{min,a}$. Heat curves $b$ and $c$ emphasize the difference between heat curve gradients.

535 with positive numbers. The buildings with decentral HPs are marked by blue crosses.

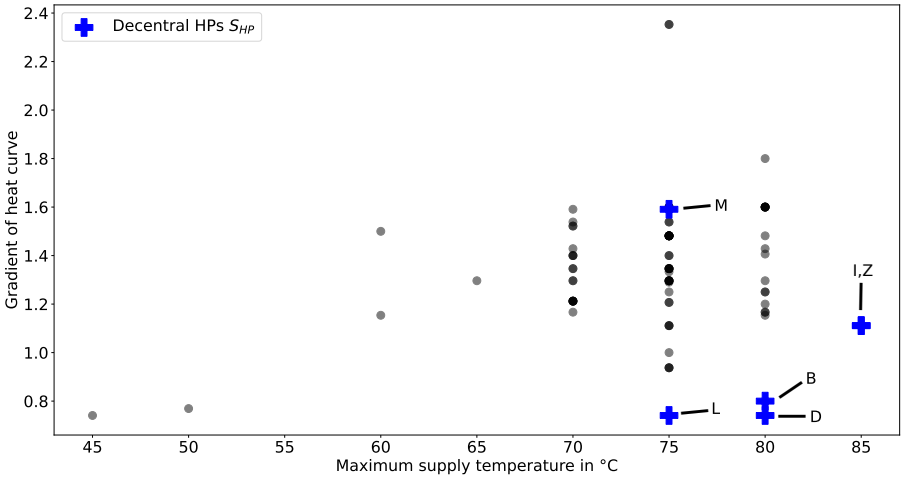



Figure 8: Gradient and design supply temperatures of the heat curves of all buildings. Buildings with a decentral HP installation in scenario $S_{HP,15}$ are marked.

It can be seen that almost all the decentral HPs are installed at buildings

with high design supply temperatures ($T^{DEM}_{in,design}$) and a low gradient of the heat curve. These heat curves are shown schematically in Figure 7 as heat curve $b$, which is outlined with a low gradient. As explained earlier in relation to Figure 7, this type of heat curve also tends towards high supply temperatures at high ambient temperatures. However, to achieve the lowest possible network temperatures for efficient waste heat utilisation at all ambient temperatures, these unfavourable heat curves of the critical buildings must be addressed by HP installation.

Besides this, one HP is installed at building M with a supply temperature of 75 °C and a high heat curve gradient of 1.7. The heat curve of this building has a design ambient temperature $T_{amb,design}$ of -2 °C, which results in high supply temperatures for relatively high ambient temperatures regardless of the heat curve gradient. See example heat curve $a$ in Figure 7 for comparison. The installation of a decentral HP at this building shows that it is essential to consider the whole heat curve and not only design supply temperatures to identify critical buildings within the existing DH network.

*DH design of $S_{Refurb,15}$*

Due to the refurbished buildings, the heat demand of the DH system is lower than in $S_{HP,15}$, resulting in a higher share of WH supply since the HS has to support less. Figure 9 presents the DH system design of scenario $S_{Refurb,15}$. It can be seen that all but one of the buildings with a decentral HP in $S_{HP,15}$ are also adapted in $S_{Refurb,15}$. In $S_{Refurb,15}$, the buildings are refurbished or still have a decentral HP. The results confirm that these are the critical buildings in the DH system that need to be adapted with any measure in order to reduce the overall DH supply temperature.

Notably, no result of scenario $S_{Refurb}$ shows a simultaneous refurbishment and installation of a decentral HP (see Table A.7), although this would be a feasible solution to the optimisation problem. The refurbishment of a building already reduces the supply temperature $T^{DEM}_{in,t}$ to such an extent that an additional HP installation becomes obsolete. Furthermore, the refurbishment

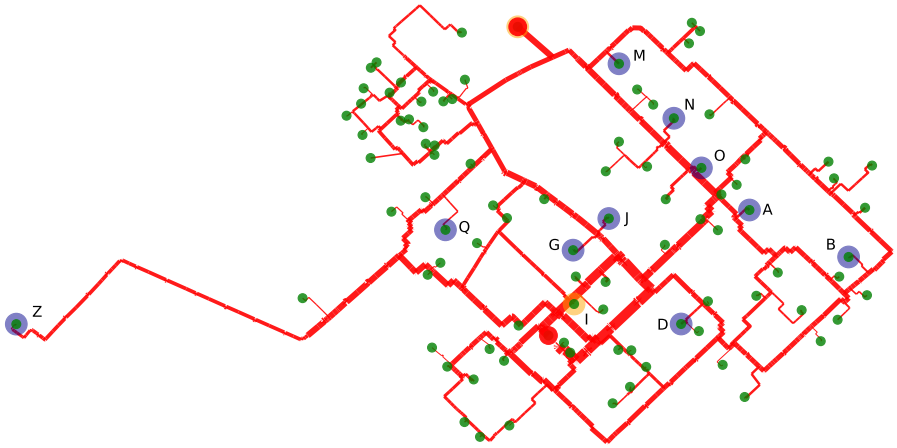



Figure 9: DH system design of scenario $S_{Refurb,15}$. Dark blue marked buildings represent the refurbishment package $\text{Refurb}_{\text{Full}}$. The refurbishment package $\text{Refurb}_{\text{Win}}$ is not applied.

package $\text{Refurb}_{\text{Win}}$ is not included in $S_{Refurb,15}$.

Figure 10 highlights the adapted buildings of scenario $S_{Refurb,15}$ with respect to the gradients of the heat curves and the design supply temperatures. Refurbished buildings are marked with red dots and buildings with only decentral HPs are marked with blue crosses.

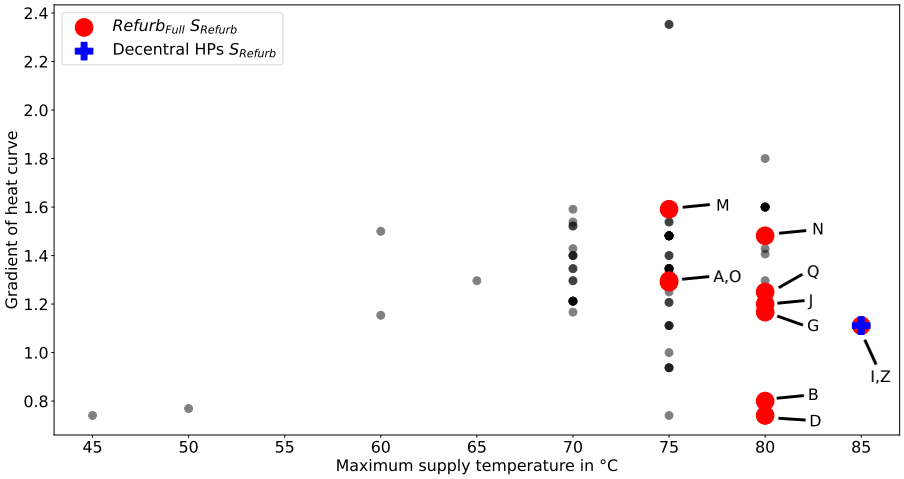



Figure 10: Gradient and design supply temperatures of the heat curves of all buildings. Decentral HP installations and applied refurbishments in scenario $S_{Refurb,15}$ are marked.

Figure 10 shows that for $S_{Refurb,15}$ the gradient of the heat curve does not influence the refurbishment decision to the same extent as decentral HP installation for $S_{HP,15}$. However, the refurbishment decisions are strongly coupled with the refurbishment cost relative to the saved heat demand. The building adaption results of $S_{Refurb,15}$ are shown in Figure 11 with the relative refurbishment costs of the refurbishment package $\text{Refurb}_{\text{Full}}$ on the y-axis and the design supply temperature on the x-axis.

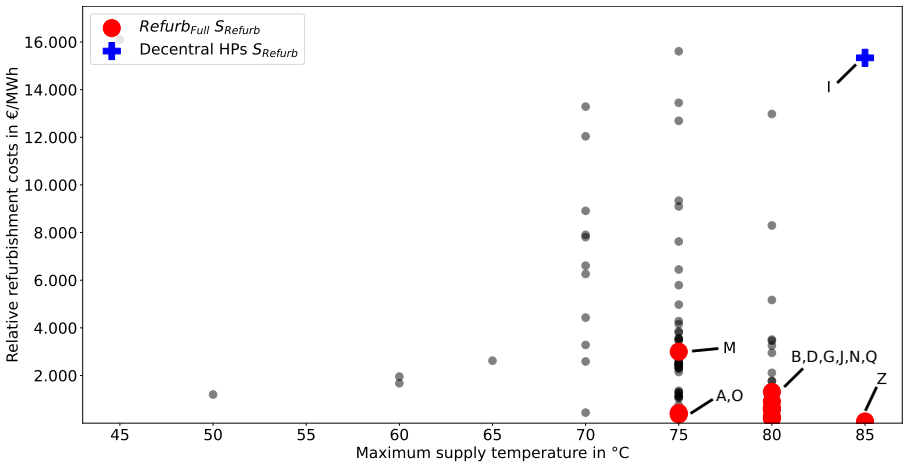



Figure 11: Relative refurbishment costs and design supply temperatures of all buildings. Decentral HP installations and applied refurbishments in scenario $S_{Refurb,15}$ are marked.

Figure 11 shows that buildings with high supply temperatures and low relative refurbishment costs are prioritised for refurbishment. Due to high relative refurbishment costs, the building shown in the upper right corner of Figure 11 is equipped with a decentral HP and is not refurbished.

*Mass flow limitations*

The optimisation provides results for the required mass flows at the supplied buildings. These required mass flows are compared with the maximum allowed mass flows in the pipe connecting the corresponding building in the DH network, i.e. the mass flow actually required for the heat supply is compared with the mass flow limit value given by the existing pipe diameter at the supplied building

(see Subsection 2.2.1).

Overall, 15 of 92 supplied buildings exceed the calculated mass flow limit in scenario $S_{Refurb,15}$. However, the mass flow of only 7 buildings, representing 8 % of the building stock, exceed the estimated limit by more than 30 %. Only one building exceeds the mass flow limit after refurbishment. The same buildings are also affected in scenario $S_{HP,15}$ with the same magnitude, but three buildings additionally exceed the mass flow limit.

Minor exceedances of the mass flow limit result in only slightly higher pressure losses in the pipes. Since the building connecting pipes are usually relatively short in length, this results in low absolute pressure losses and can therefore be tolerated in most cases. Nevertheless, a few connecting pipes have more critical pressure losses due to the mass flow limits with the most critical pipe exceeding the limit by 75 %. If the proposed DH transformation design would be realised, such critical pipes need to be further investigated, as these pipe segments may lead to avoidable high absolute pressure losses or high material stresses. However, since only the DH mass flows at the buildings are known from the optimisation model, the mass flow analysis only relates to the building connecting pipes, but not to other pipe segments in the network.

*Energy analysis*

The typical days determined for the operational optimisation (see Section 3) are used to present an energy analysis of the transformed DH system. Figure 12 shows the ten typical days on the x-axis. The ambient air temperature $T_{amb,t}$ of these ten days is presented in the lower part of the figure. The energy flows of scenario $S_{HP,15}$ and $S_{Refurb,15}$ are shown in the top and centre section of Figure 12.

It can be seen that the use of the existing heating station $\dot{Q}_{HS}$ is significantly reduced in scenario $S_{Refurb,15}$ compared to scenario $S_{HP,15}$. The reduced peak load during winter days results from the refurbishment of some buildings, which reduces the overall heat demand of the DH system. The reduced heat demand can be observed on nearly every typical day except some summer days. In

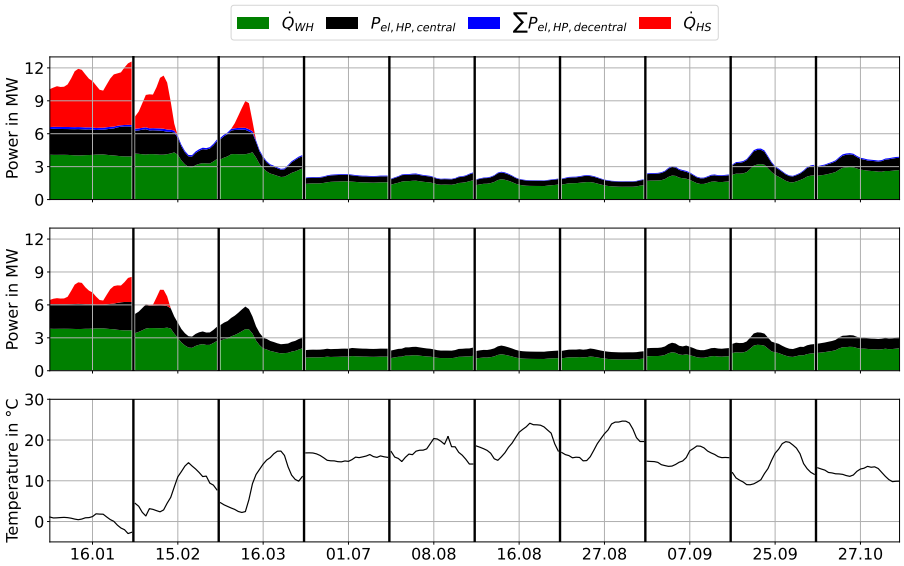



Figure 12: Energy analysis for each typical day. Scenario $S_{HP,15}$ is shown in the upper part and scenario $S_{Refurb,15}$ is shown in the middle part. The lower part shows the ambient air temperature $T_{amb,t}$.

addition, the electricity consumption for operating the decentral HPs in scenario $S_{Refurb,15}$ is close to zero, as the refurbishment of the buildings minimises the need to install decentral HPs. Due to the reduced heat supply from the existing heating station $\dot{Q}_{HS}$ between the scenarios, the proportion of waste heat on DH supply increases, especially on days with high heat demand. On the 16th of January, the proportion of waste heat for $S_{Refurb,15}$ reaches 52.5 %, while on the same day the waste heat proportion for the scenario $S_{HP,15}$ is only 36.8 %.

Based on the energy analysis, the impact on $CO_2$ emissions for both scenarios is briefly described. By assuming $CO_2$ factors for the different energy sources, the $CO_2$ emissions can be calculated for both scenarios. Table 3 shows the different $CO_2$ factors for consumed electricity and supply by the existing HS as well as the total emissions for each scenario. The $CO_2$ impact of waste heat usage is neglected.

Scenario $S_{HP,15}$ leads to slightly higher emissions in electricity consumption but to significantly higher emissions due to the heat supply of the HS, so scenario

Table 3: $CO_2$ emission factors and $CO_2$ emissions for each energy source and scenario.

| | Electricity | HS supply | total |
|---|---|---|---|
| $CO_2$ factor in kg/MWh | 78.58 | 234.88 | - |
| $CO_2$ emissions of $S_{HP,15}$ in t/a | 2,931 | 4,537 | 7,468 |
| $CO_2$ emissions of $S_{Refurb,15}$ in t/a | 2,721 | 494 | 3,215 |

$S_{Refurb,15}$ is more favourable in terms of reducing $CO_2$ emissions. Therefore, scenario $S_{Refurb,15}$ shows lower $CO_2$ emissions and also lower TAC compared to scenario $S_{HP,15}$ (see also Figure 5). This underlines the necessary consideration of refurbishment options as part of the DH transformation process, as the economic and environmental impacts are more favourable than if only HP installation would be considered as done in scenario $S_{HP,15}$.

*4.2.2. Operational optimisation*

The second stage of the optimisation, the operational optimisation, is performed with ten typical days (see Section 3) and solved with the same solver settings as the design optimisation. The results of the design optimisation (see Section 4.2) are used to fix the design variables. To optimise the DH operation, the previously fixed $\Delta T^{NET,b}$ of the network is assumed to be a variable over time. The results are shown in Figure 13, the network temperatures for a variable $\Delta T_t^{NET,b}$ in the upper part and the corresponding ambient temperature of the typical days in the lower part. For comparison, the middle part of Figure 13 shows the network temperatures for a fixed $\Delta T^{NET,b}$, i.e. an operational optimisation with fixed design variables and a constant $\Delta T^{NET,b}$.

For the fixed $\Delta T^{NET,b}$ in the middle graph, it can be seen that the supply temperature $T_{in,t}^{NET,a}$ of the DH network is higher in the winter and lower in the summer. Furthermore, the relative temperature difference between $T_{in,t}^{NET,a}$ and $T_{out,t}^{NET,b}$ at the heat sources is lower in the winter and higher in the summer. Due to the higher heat demand in winter, the network mass flow is higher

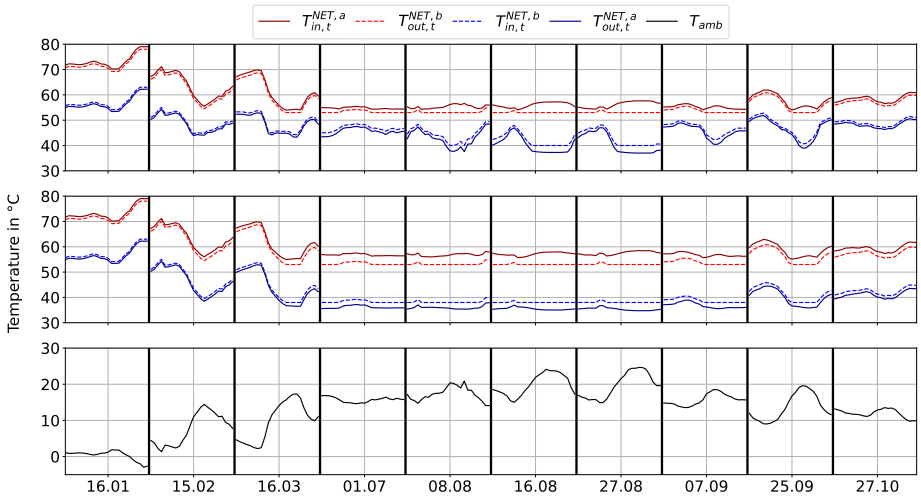



Figure 13: Operational results for each typical day of scenario $S_{HP,15}$. The upper part shows the network temperatures of the DH system with a variable $\Delta T_t^{NET,b}$ and the middle part with a fixed $\Delta T^{NET,b}$ of 15 K. The lower part of the figure shows the ambient air temperature $T_{amb,t}$.

and therefore the relative heat losses are lower than in summer. A network temperature $T_{out,t}^{NET,b}$ of 53 °C at the days 01.07 to 07.09 results from a required supply temperature $T_{in,t}^{DEM}$ of 50 °C of at least one building connected via a HX.

For a variable $\Delta T_t^{NET,b}$, the results show a 1.04 % lower TAC compared to the results with a fixed $\Delta T^{NET,b}$ of 15 K. In the upper graph of Figure 13, it can be seen that the relative heat losses, indicated by the temperature difference between $T_{in,t}^{NET,a}$ and $T_{out,t}^{NET,b}$, are lower in the summer days compared to the results with a fixed $\Delta T^{NET,b}$. This is due to a lower $\Delta T_t^{NET,b}$ in summer, which leads to higher mass flows and therefore to smaller relative heat losses. However, $\Delta T_t^{NET,b}$ does not increase above 15 K on winter days, although it is possible. Increasing $\Delta T_t^{NET,b}$ would result in an increased network temperature $T_{out,t}^{NET,b}$ due to the operational constraints of the HX and a fixed temperature difference of the SH system $\Delta T^{DEM}$ of 15 K at the building side of the HX. An increased network temperature $T_{out,t}^{NET,b}$ would result in a higher power consumption of the central HP and therefore to higher TAC. Instead, the mass flows are

increased and the temperature difference $\Delta T_t^{NET,b}$ is set to 15 K to meet the temperature requirements and heat supply of the HX-supplied buildings during highest demands.

Compared to the reference scenario $S_{Ref,15}$ with only one central HP, scenario $S_{HP,15}$ reduces the network temperature $T_{in,t}^{NET,a}$ by about 5 K at nominal heating loads and up to 11 K on summer days. Compared to the current operating data of the real HTDH system, the maximal supply temperature is reduced from 130 °C to 80 °C. Therefore, the DH transformation of the HTDH system, including design and operational optimisation, does not achieve a holistic reduction in supply temperatures to 70 °C, although the supply temperature are mostly in the range of typical LTDH systems.

The operational optimisation of scenario $S_{Refurb,15}$ shows similar temperature reductions as $S_{HP,15}$ at nominal heating loads, but higher network temperatures on summer days. The higher network temperatures are due to a supplied building that still has a high supply temperature requirement of 60 °C in summer even after refurbishment. Since no HP installation is part of the optimal solution at this building, these high temperature requirements must be met directly by the DH network.

Overall, the additional performed operational optimisation demonstrates the ability to increase the efficiency of the transformed DH design by further reducing network temperatures and operating costs.

## 5. Discussion

This section discusses the presented methods and the obtained results. The simulation of refurbishment measures as well as the optimisation model are discussed, followed by a critical discussion about the changed mass flow conditions in the network due to the transformation.

### *5.1. Analysed case study*

The analysed HTDH system supplies almost one hundred non-residential buildings at a research facility. Due to the characteristics of the buildings pre-

sented, the heat curves are very individual, which also influences the measures applied when optimising the DH transformation as discussed in Section 4.2.1. In other DH systems with a more homogeneous building stock, the heat curves might not differ so much, so the heating system design temperature is more important for decisions on refurbishment and HP installation than the gradients of the heat curves.

In the case study presented, there is no domestic hot water demand in the buildings, or it is covered by an alternative electric heating system. However, if the domestic hot water demand of a building is also covered by a DH system, e.g. in DH systems that mainly supply residential buildings, the temperature requirements of the hot water demand to prevent legionella growth can also influence the decision of DH transformation measure.

### *5.2. Simulation of refurbishment measures*

The impact of refurbishment packages on existing buildings in the DH system is derived from generic simulation models that are parameterised with minimal input data as detailed information for each existing building in the DH system is not available. The degree of uncertainty of this approach to estimate the impact of generic simulation models as opposed to detailed simulation models for each individual building could not be addressed in this study and should be the subject of future work. Nonetheless, the results of simulation models created with *TEASER* show minor deviations in relation to the heat demand measurements when analysing the entire district as shown in [39]. Small deviations also apply to this study, as the estimated effects of the refurbishment measures on heating load and supply temperatures (see Section 4.1) are comparable to similar studies. Brand et al. [28] showed that the supply temperature $T^{DEM}_{in,design}$ of a 1970 Danish single-family building can be reduced by 20 to 45 %, depending on the extent of refurbishment. Harrestrup et al. [27] investigated two Danish multi-family buildings from the 1900's and showed that the nominal heating load $\dot{Q}^{DEM}_{nominal}$ can be reduced by 52 to 72 % in the case of a comprehensive refurbishment and by 15 to 30 % in the case of a window refurbishment. The

simulation results from this case study show similar results for buildings built between 1960 and 1980, with average reductions in nominal heating load and supply temperature of 45 to 9 % and 30 to 5 %, respectively.

Since the evaluation of refurbishment measures on the supplied buildings is based on minimal input data and assumptions about the SH systems, the actual reductions in heating load and SH supply temperature may differ from the estimations. However, the obtained results of the refurbishment effects help to identify the most beneficial refurbishment potentials for the transformation of the entire DH system.

### *5.3. Performance of the optimisation model*

Scenarios $S_{HP}$ considering only the installation of decentral HPs show optimality gaps below 1 %, while the scenarios considering also refurbishment measures $S_{Refurb}$ show gaps between 1.7 % and 22.3 %. The consideration of optional refurbishment states in $S_{Refurb}$ for each supplied building adds multiple binary variables to the optimisation model and thus increases the computational time of the design optimisation. Gaps of 1.7 % can already demonstrate the potential of the model formulation with optional refurbishment states, however, larger DH systems than the one studied lead to larger models and thus to extended computational time. Therefore, the performance of the presented optimisation model, especially the consideration of two refurbishment states for each building, needs to be evaluated for larger DH systems.

### *5.4. Increasing mass flows*

The DH design with the lowest TAC is determined with a $\Delta T^{NET,b}$ of 15 K, which is much lower than the previous HTDH temperature difference and therefore leads to increasing mass flows that may even exceed the estimated limits. Guelpa et al. [8] described that when integrating a low-temperature heat source into an existing DH system, the mass flow limits of the existing pipe network should be exploited due to reduced network temperatures. However, the replacement of most critical pipes, which would otherwise lead to high total pressure

losses, should be considered as part of the faced DH transformation. A simulative assessment of the adapted DH system design and its operating temperatures to evaluate the mass flow conditions in the network structure, similar to [15], should be the subject of future work. Thus, the most critical pipe segments could be identified more accurately and necessary pipe replacements derived.

## 6. Conclusion

The integration of sustainable low-temperature heat sources into existing DH systems decarbonises the heat supply of buildings but requires action at different system levels to balance heat source and network temperatures. This paper presents a methodology to optimise the transformation of existing DH systems to enhance the integration of low-temperature heat sources, taking into account the installation of central and decentral HPs and the optional refurbishment of supplied buildings. The sole replacement of windows and a full refurbishment of the building envelope are evaluated using building simulation models. Based on a comparison of the simulation results, refurbishment packages for the existing buildings are derived that include individual heating load and SH supply temperature reductions. Building refurbishment and HP installation decisions are integrated into a design optimisation for the DH system transformation. Subsequently, an operational optimisation with fixed design decisions calculates the optimal operating conditions of the transformed DH system.

The presented methodology is applied to a real-world HTDH system with an intended waste heat integration at low-temperature level. The design optimisation shows that buildings with high SH supply temperatures, unfavourable heat curve designs and low refurbishment costs are adapted to transform the DH system. By considering optional building refurbishment and decentral HP installation in the optimisation model, the TAC could be reduced by up to 24.4 % compared to only incorporating one central HP for waste heat integration. The subsequent operational optimisation shows the potential to further increase the DH system efficiency by reducing heat losses and thereby reduc-

ing operating costs. Although the present work focuses on the integration of a low-temperature heat source, the developed model could also be used for DH transformation without additional heat source integration but with the intention to reduce the supply temperatures in the network to enable more efficient DH operation.

For future work, a simulative assessment of the obtained DH system design should be performed, as the mass flow conditions in the network structure need to be evaluated in more detail. Overall, the presented methodology demonstrates the potential to obtain optimal design and operation of transformed HTDH systems with efficient integration of low-temperature heat sources, while considering options for HP installations and refurbishment of supplied buildings.

## Author Contributions

**Jan Stock**: Conceptualization, Methodology, Investigation, Validation, Writing - Original Draft, Writing - Review and Editing, Visualization. **Till Schmidt**: Methodology, Investigation, Software, Writing - Original Draft, Writing - Review and Editing, Visualization. **André Xhonneux**: Supervision, Writing - Review and Editing, Project administration, Funding acquisition, Resources. **Dirk Müller**: Writing - Review and Editing, Project administration, Funding acquisition, Resources.

## Declaration of competing interest

The authors declare that they have no known competing financial interests or personal relationships that could have appeared to influence the work reported in this paper.

## Acknowledgements

This work was supported by the Helmholtz Association under the project "Helmholtz platform for the design of robust energy systems and their supply

chains" (RESUR).

## Nomenclature

### Abbreviations

| | |
|---|---|
| CAPEX | Capital Expenditures |
| DEM | Demand |
| DH | District Heating |
| HP | Heat Pump |
| HS | Heating Station |
| HTDH | High Temperature District Heating |
| HX | Heat Exchanger |
| LC | Linking Component |
| LTDH | Low-Temperature District Heating |
| MILP | Mixed Integer Linear Programming |
| MIQCP | Mixed Integer Quadraticly Constrained Programming |
| NET | Network |
| OPEX | Operational Expenditures |
| PG | Power Grid |
| Ref | Reference Scenario |
| Refurb | Refurbishment |
| SH | Space Heating |
| TAC | Total Annualized Costs |
| WH | Waste Heat |

### Symbols

| | |
|---|---|
| $\Delta$ | Difference, - |
| $\dot{Q}$ | Heat Flow, W |
| $\dot{m}$ | Mass Flow, kg/s |
| $b$ | Binary Variable, - |

| | |
|---|---|
| $I$ | Investment, EUR |
| $p$ | Specific Price, EUR/kWh |
| $T$ | Temperature, K |
| $w$ | Weighting Factor, - |

**Indices and Sets**

| | |
|---|---|
| $c \in C$ | Consumer of DH system |
| $t \in T$ | Timestep |

**Subscripts and Superscripts**

| | |
|---|---|
| $a$ | Component Side a |
| $amb$ | Ambient |
| $avg$ | Average |
| $b$ | Component Side b |
| $el$ | Electricity |
| $i$ | Interest Rate |
| $in$ | Input |
| $log$ | Logarithmic |
| $n$ | Time Horizon |
| $nom$ | Nominal |
| $out$ | Output |
| $ret$ | Return |
| $sup$ | Supply |
| $spec$ | Specific |
| $win$ | Windows |

## References

[1] European Comission, The european green deal investment plan and just transition mechanism explained (2020).

URL https://ec.europa.eu/commission/presscorner/detail/en/qanda_20_24

[2] European Union, Eu energy in figures, Statistical pocketbook 2022 (2022). URL https://op.europa.eu/en/publication-detail/-/publication/7d9ae428-3ae8-11ed-9c68-01aa75ed71a1/language-en

[3] eurostat, Energy consumption in households (2020). URL https://ec.europa.eu/eurostat/statistics-explained/index.php?title=Energy_consumption_in_households

[4] A. M. Jodeiri, M. J. Goldsworthy, S. Buffa, M. Cozzini, Role of sustainable heat sources in transition towards fourth generation district heating – a review, Renewable and Sustainable Energy Reviews 158 (2022) 112156. doi:10.1016/j.rser.2022.112156.

[5] R. Lund, U. Persson, Mapping of potential heat sources for heat pumps for district heating in denmark, Energy 110 (2016) 129–138. doi:10.1016/j.energy.2015.12.127.

[6] P. Huang, B. Copertaro, X. Zhang, J. Shen, I. Löfgren, M. Rönnelid, J. Fahlen, D. Andersson, M. Svanfeldt, A review of data centers as prosumers in district energy systems: Renewable energy integration and waste heat reuse for district heating, Applied Energy 258 (2020) 114109. doi:10.1016/j.apenergy.2019.114109.

[7] H. Lund, S. Werner, R. Wiltshire, S. Svendsen, J. E. Thorsen, F. Hvelplund, B. V. Mathiesen, 4th generation district heating (4gdh), Energy 68 (2014) 1–11. doi:10.1016/j.energy.2014.02.089.
URL https://www.sciencedirect.com/science/article/pii/S0360544214002369

[8] E. Guelpa, M. Capone, A. Sciacovelli, N. Vasset, R. Baviere, V. Verda, Reduction of supply temperature in existing district heating: A review of

strategies and implementations, Energy 262 (2023) 125363. doi:10.1016/j.energy.2022.125363.

[9] H. Averfalk, S. Werner, Essential improvements in future district heating systems, Energy Procedia 116 (2017) 217–225. doi:10.1016/j.egypro.2017.05.069.

[10] H. Li, N. Nord, Transition to the 4th generation district heating - possibilities, bottlenecks, and challenges, Energy Procedia 149 (2018) 483–498. doi:10.1016/j.egypro.2018.08.213.

[11] J. Formhals, F. Feike, H. Hemmatabady, B. Welsch, I. Sass, Strategies for a transition towards a solar district heating grid with integrated seasonal geothermal energy storage, Energy 228 (2021) 120662. doi:10.1016/j.energy.2021.120662.

[12] B. Kleinertz, K. Gruber, District heating supply transformation – strategies, measures, and status quo of network operators' transformation phase, Energy 239 (2022) 122059. doi:10.1016/j.energy.2021.122059.

[13] A. Volkova, V. Mašatin, A. Siirde, Methodology for evaluating the transition process dynamics towards 4th generation district heating networks, Energy 150 (2018) 253–261. doi:10.1016/j.energy.2018.02.123.

[14] N. Nord, M. Shakerin, T. Tereshchenko, V. Verda, R. Borchiellini, Data informed physical models for district heating grids with distributed heat sources to understand thermal and hydraulic aspects, Energy 222 (2021) 119965. doi:10.1016/j.energy.2021.119965.

[15] J. Stock, F. Arjuna, A. Xhonneux, D. Müller, Modelling of waste heat integration into an existing district heating network operating at different supply temperatures, Smart Energy 10 (2023) 100104. doi:10.1016/j.segy.2023.100104.
URL https://www.sciencedirect.com/science/article/pii/S2666955223000114

[16] J. Oltmanns, D. Sauerwein, F. Dammel, P. Stephan, C. Kuhn, Potential for waste heat utilization of hot–water–cooled data centers: A case study, Energy Science & Engineering 8 (5) (2020) 1793–1810. doi:10.1002/ese3.633.

[17] H. Dorotić, K. Čuljak, J. Miškić, T. Pukšec, N. Duić, Technical and economic assessment of supermarket and power substation waste heat integration into existing district heating systems, Energies 15 (5) (2022) 1666. doi:10.3390/en15051666.

[18] P. A. Østergaard, A. N. Andersen, Booster heat pumps and central heat pumps in district heating, Applied Energy 184 (2016) 1374–1388. doi:10.1016/j.apenergy.2016.02.144.

[19] M. Rämä, K. Sipilä, Transition to low temperature distribution in existing systems, Energy Procedia 116 (2017) 58–68. doi:10.1016/j.egypro.2017.05.055.

[20] H. İ. Topal, H. İ. Tol, M. Kopaç, A. Arabkoohsar, Energy, exergy and economic investigation of operating temperature impacts on district heating systems: Transition from high to low-temperature networks, Energy 251 (2022) 123845. doi:10.1016/j.energy.2022.123845.

[21] A. Reguis, B. Vand, J. Currie, Challenges for the transition to low-temperature heat in the uk: A review, Energies 14 (21) (2021) 7181. doi:10.3390/en14217181.

[22] M. Tunzi, D. S. Østergaard, S. Svendsen, R. Boukhanouf, E. Cooper, Method to investigate and plan the application of low temperature district heating to existing hydraulic radiator systems in existing buildings, Energy 113 (2016) 413–421. doi:10.1016/j.energy.2016.07.033.

[23] D. S. Østergaard, K. M. Smith, M. Tunzi, S. Svendsen, Low-temperature operation of heating systems to enable 4th generation district heating: A review, Energy 248 (2022) 123529. doi:10.1016/j.energy.2022.123529.

[24] H. Lund, P. A. Østergaard, M. Chang, S. Werner, S. Svendsen, P. Sorknæs, J. E. Thorsen, F. Hvelplund, B. O. G. Mortensen, B. V. Mathiesen, C. Bojesen, N. Duic, X. Zhang, B. Möller, The status of 4th generation district heating: Research and results, Energy 164 (2018) 147–159. doi:10.1016/j.energy.2018.08.206.

[25] D. S. Østergaard, S. Svendsen, Replacing critical radiators to increase the potential to use low-temperature district heating – a case study of 4 danish single-family houses from the 1930s, Energy 110 (2016) 75–84. doi:10.1016/j.energy.2016.03.140.

[26] M. Lämmle, C. Bongs, J. Wapler, D. Günther, S. Hess, M. Kropp, S. Herkel, Performance of air and ground source heat pumps retrofitted to radiator heating systems and measures to reduce space heating temperatures in existing buildings, Energy 242 (2022) 122952. doi:10.1016/j.energy.2021.122952.

[27] M. Harrestrup, S. Svendsen, Changes in heat load profile of typical danish multi-storey buildings when energy-renovated and supplied with low-temperature district heating, International Journal of Sustainable Energy 34 (3-4) (2015) 232–247. doi:10.1080/14786451.2013.848863.

[28] M. Brand, S. Svendsen, Renewable-based low-temperature district heating for existing buildings in various stages of refurbishment, Energy 62 (2013) 311–319. doi:10.1016/j.energy.2013.09.027.

[29] Q. Wang, A. Ploskić, S. Holmberg, Retrofitting with low-temperature heating to achieve energy-demand savings and thermal comfort, Energy and Buildings 109 (2015) 217–229. doi:10.1016/j.enbuild.2015.09.047.

[30] D. Hering, A. Xhonneux, D. Müller, Design optimization of a heating network with multiple heat pumps using mixed integer quadratically constrained programming, Energy 226 (2021) 120384. doi:10.1016/j.energy.2021.120384.

[31] C. Mateu-Royo, S. Sawalha, A. Mota-Babiloni, J. Navarro-Esbrí, High temperature heat pump integration into district heating network, Energy Conversion and Management 210 (2020) 112719. doi:10.1016/j.enconman.2020.112719.

[32] M. Capone, E. Guelpa, V. Verda, Optimal installation of heat pumps in large district heating networks, Energies 16 (3) (2023) 1448. doi:10.3390/en16031448.

[33] B. Bach, J. Werling, T. Ommen, M. Münster, J. M. Morales, B. Elmegaard, Integration of large-scale heat pumps in the district heating systems of greater copenhagen, Energy 107 (2016) 321–334. doi:10.1016/j.energy.2016.04.029.

[34] M. Sameti, F. Haghighat, Optimization approaches in district heating and cooling thermal network, Energy and Buildings 140 (2017) 121–130. doi:10.1016/j.enbuild.2017.01.062.

[35] M. Wirtz, M. Hahn, T. Schreiber, D. Müller, Design optimization of multi-energy systems using mixed-integer linear programming: Which model complexity and level of detail is sufficient?, Energy Conversion and Management 240 (2021) 114249. doi:10.1016/j.enconman.2021.114249.

[36] M. Capone, E. Guelpa, V. Verda, Multi-objective optimization of district energy systems with demand response, Energy 227 (2021) 120472. doi:10.1016/j.energy.2021.120472.

[37] D. Hering, M. R. Faller, A. Xhonneux, D. Müller, Operational optimization of a 4th generation district heating network with mixed integer quadratically constrained programming, Energy 250 (2022) 123766. doi:10.1016/j.energy.2022.123766.

[38] J. Wasserfall, M. Powilleit, S. Kirschbaum, G. Wrobel, Efficient formulation for optimizing temperature dependent energy systems with mixed-integer quadratically constrained programming, in: Wojciech Stanek, P. Gładysz,

Sebastian Werle, Wojciech Adamczyk (Ed.), Proceedings of ECOS 2019: The 32nd International Conference on Efficiency, Cost, Optimization, Simulation and Environmental Impact of Energy Systems, 2019, pp. 953–965.

[39] P. Remmen, M. Lauster, M. Mans, M. Fuchs, T. Osterhage, D. Müller, Teaser: an open tool for urban energy modelling of building stocks, Journal of Building Performance Simulation 11 (1) (2018) 84–98. doi:10.1080/19401493.2017.1283539.

[40] B. Oschatz, Kosten energierelevanter bau- und technischer anlagenteile bei der energetischen sanierung von nichtwohngebäuden/ bundesliegenschaften (2014).

[41] H. Pieper, T. Ommen, F. Buhler, B. L. Paaske, B. Elmegaard, W. B. Markussen, Allocation of investment costs for large-scale heat pumps supplying district heating, Energy Procedia 147 (2018) 358–367. doi:10.1016/j.egypro.2018.07.104.

[42] M. Langiu, D. Y. Shu, F. J. Baader, D. Hering, U. Bau, A. Xhonneux, D. Müller, A. Bardow, A. Mitsos, M. Dahmen, Comando: A next-generation open-source framework for energy systems optimization, Computers & Chemical Engineering 152 (11) (2021) 107366. doi:10.1016/j.compchemeng.2021.107366.
URL http://arxiv.org/pdf/2102.02057v2

[43] T. Nussbaumer, S. Thalmann, Influence of system design on heat distribution costs in district heating, Energy 101 (2016) 496–505. doi:10.1016/j.energy.2016.02.062.

[44] D. Thiel, M. Ehrlich, Ermittlung von spezifischen kosten energiesparender bauteil-, beleuchtungs-, heizungs- und klimatechnikausführungen bei nichtwohngebäuden für die wirtschaftlichkeitsuntersuchungen zur enev 2012: Bmvbs-online-publikation.

[45] M. Fuchs, J. Teichmann, M. Lauster, P. Remmen, R. Streblow, D. Müller, Workflow automation for combined modeling of buildings and district energy systems, Energy 117 (2016) 478–484. doi:10.1016/j.energy.2016.04.023.
URL https://www.sciencedirect.com/science/article/pii/S0360544216304297

[46] Statistisches Bundesamt, Statistisches bundesamt (destatis), genesis-online (2023).
URL https://www-genesis.destatis.de/genesis/online

[47] L. Kotzur, L. Nolting, M. Hoffmann, T. Groß, A. Smolenko, J. Priesmann, H. Büsing, R. Beer, F. Kullmann, B. Singh, A. Praktiknjo, D. Stolten, M. Robinius, A modeler's guide to handle complexity in energy systems optimization, Advances in Applied Energy 4 (2021) 100063. doi:10.1016/j.adapen.2021.100063.
URL https://www.sciencedirect.com/science/article/pii/S266679242100055X

[48] T. Schütz, D. Müller, H. Harb, M. H. Schraven, M. Fuchs, Clustering algorithms for the selection of typical demand days for the optimal design of building energy systems, Proceedings of ECOS 2016 2016 (Proceedings of ECOS 2016).

[49] F. Dominguez-Munoz, J. M. Cejudo-Lopez, A. Carrillo-Andres, M. Gallardo-Salazar, Selection of typical demand days for chp optimization, Energy and Buildings (2011).

[50] Gurobi Optimization, Gurobi optimization llc. gurobi optimizer reference manual.
URL https://www.gurobi.com

## Appendix A. Appendix

Table A.4: Cost functions of refurbishment measures according to Ref. [40].

| Refurbishment measure | Cost function | Parameter |
|---|---|---|
| Window exchange | $(\mathrm{A_{win}} \ / \ \mathrm{A_{mean}}) \cdot \Big[ 180 \cdot \mathrm{A_{mean}} + 75 \cdot 4 \cdot \sqrt{A_{\mathrm{mean}}} + 35 + 19 \cdot \mathrm{A_{mean}} \Big]$ | $\mathrm{A_{mean}} = 1.8\mathrm{m}^2$ |
| Wall insulation | $(\lambda_{ins} \ / \ 0.035) \cdot \Big[ \mathrm{A_{Wall}} \cdot (75 + 1.9 \cdot \mathrm{d_{ins}}) \Big]$ | $\lambda_{ins} = 0.041$ W/mK, $d_{ins} = 12$ cm |
| Roof insulation | $(\lambda_{ins} \ / \ 0.035) \cdot \Big[ \mathrm{A_{Roof}} \cdot (25 + 1.8 \cdot \mathrm{d_{ins}}) \Big]$ | $\lambda_{ins} = 0.041$ W/mK, $d_{ins} = 12$ cm |
| Ground floor insulation | $(\lambda_{ins} \ / \ 0.035) \cdot \Big[ \mathrm{A_{Floor}} \cdot (45 + 1.8 \cdot \mathrm{d_{ins}}) \Big]$ | $\lambda_{ins} = 0.041$ W/mK, $d_{ins} = 12$ cm |
| Framework | $7.6 \cdot \mathrm{A_{Wall}} + 326$ | - |
| Radiator exchange | $(240 \cdot (0.1 \cdot \dot{Q}_{nominal})) + 140$ | - |

Table A.5: Results of $S_{HP}$ design optimisations for different $\Delta T^{NET,b}$ values.

| Parameters | 10 | 11 | 12 | 13 | 14 | 15 | 16 | 17 | 18 | 19 | 20 | 21 | 22 | 23 | 24 | 25 |
|---|---|---|---|---|---|---|---|---|---|---|---|---|---|---|---|---|
| TAC [TEUR] | 6,432 | 6,047 | 5,680 | 5,363 | 5,163 | 4,950 | 4,967 | 4,987 | 5,010 | 5,084 | 5,208 | 5,308 | 5,421 | 5,534 | 5,648 | 5,761 |
| GAP [%] | 0 | 0.03 | 1 | 0.99 | 1 | 1 | 0.98 | 0.98 | 1 | 0.98 | 0.97 | 0.8 | 0.39 | 0.96 | 0.71 | 0.67 |
| # HPs | 92 | 92 | 92 | 92 | 13 | 7 | 7 | 7 | 7 | 7 | 9 | 7 | 7 | 7 | 7 | 7 |

Table A.6: Results of $S_{Refurb}$ design optimisations for different $\Delta T^{NET,b}$ values.

| Parameters | 10 | 11 | 12 | 13 | 14 | 15 | 16 | 17 | 18 | 19 | 20 | 21 | 22 | 23 | 24 | 25 |
|---|---|---|---|---|---|---|---|---|---|---|---|---|---|---|---|---|
| TAC [TEUR] | 4,362 | 4,226 | 4,057 | 3,977 | 4,038 | 4,000 | 4,183 | 4,257 | 4,305 | 4,374 | 4,467 | 4,662 | 4,836 | 5,016 | 5,031 | 5,154 |
| GAP [%] | 13.6 | 11.4 | 3.9 | 1.7 | 10.7 | 9.1 | 23.3 | 12.1 | 14.8 | 6.6 | 22.3 | 13.3 | 17.7 | 18.6 | 14.7 | 12.7 |
| # HPs | 92 | 3 | 2 | 2 | 3 | 2 | 1 | 2 | 2 | 2 | 2 | 4 | 5 | 6 | 2 | 4 |
| # $\text{Refurb}_{\text{Win}}$ | 0 | 0 | 0 | 0 | 1 | 0 | 1 | 8 | 1 | 0 | 0 | 0 | 1 | 3 | 0 | 1 |
| # $\text{Refurb}_{\text{Full}}$ | 10 | 16 | 17 | 15 | 10 | 10 | 13 | 14 | 17 | 15 | 13 | 12 | 8 | 9 | 8 | 3 |

Table A.7: System design of scenario $S_{HP,15}$ and $S_{Refurb,15}$.

| | $S_{HP,15}$ | $S_{Refurb,15}$ | |
|---|---|---|---|
| Building | HP sizing [kW] | HP sizing [kW] | Refurbishment |
| A | - | - | $\text{Refurb}_{\text{Full}}$ |
| B | 621.2 | - | $\text{Refurb}_{\text{Full}}$ |
| D | 806.9 | - | $\text{Refurb}_{\text{Full}}$ |
| G | - | - | $\text{Refurb}_{\text{Full}}$ |
| I | 60.7 | 60.7 | - |
| J | - | - | $\text{Refurb}_{\text{Full}}$ |
| L | 888.8 | - | - |
| M | 234.3 | - | $\text{Refurb}_{\text{Full}}$ |
| N | - | - | $\text{Refurb}_{\text{Full}}$ |
| O | - | - | $\text{Refurb}_{\text{Full}}$ |
| Q | - | - | $\text{Refurb}_{\text{Full}}$ |
| Z | 1,203.8 | - | $\text{Refurb}_{\text{Full}}$ |
| WH ($\text{HP}_{\text{central}}$) | 12,557.3 | 11,785.7 | - |